Supplementary Tables

Table S1 Strains used; all strains are congenic with the W303 background

Table S1; Strains for Genomic Analysis (RNA-seq or MNase-seq)

Strain	Analysis	Genotype
DY150	RNA, MNase	*MAT**a** ade2 can1 his3 leu2 trp1 ura3*
DY12554	RNA, MNase	*MAT**a** ade2 can1 his3 leu2 lys2 trp1 ura3 pob3(Q308K)::KanMX*
DY16281	RNA, MNase	*MAT**a** ade2 can1 his3 leu2 trp1 ura3 HHT1(K56Q) HHT2(K56Q)*
DY16302	RNA	*MAT**a** ade2 can1 his3 leu2 trp1 ura3 HHT1(K56R) HHT2(K56R)*
DY16592	RNA, MNase	*MAT**a** ade2 can1 his3 leu2 lys2 trp1 ura3 HHT1(K56Q) HHT2(K56Q) pob3(Q308K)::KanMX*
8159-4-1	RNA	*MAT**a** ade2 can1 his3 leu2 trp1 ura3 spt16(G132D)*
8315-8-1	RNA	*MAT**a** ade2 can1 his3 leu2 trp1 ura3 spt16-11*

Table S1; Strains used in Figure 2

Strain	Genotype
Top panel	
DY150	*MAT**a** ade2 can1 his3 leu2 trp1 ura3*
DY16281	*MAT**a** ade2 can1 his3 leu2 trp1 ura3 HHT1(K56Q) HHT2(K56Q)*
DY16302	*MAT**a** ade2 can1 his3 leu2 trp1 ura3 HHT1(K56R) HHT2(K56R)*
DY16313	*MAT**a** ade2 can1 his3 leu2 lys2 trp1 ura3 HHT1(K56A) HHT2(K56A)*
DY12554	*MAT**a** ade2 can1 his3 leu2 lys2 trp1 ura3 pob3(Q308K)::KanMX*
DY16592	*MAT**a** ade2 can1 his3 leu2 lys2 trp1 ura3 HHT1(K56Q) HHT2(K56Q) pob3(Q308K)::KanMX*
DY16689	*MAT**a** ade2 can1 his3 leu2 trp1 ura3 HHT1(K56R) HHT2(K56R) pob3(Q308K):KanMX*
DY17970	*MAT**a** ade2 can1 his3 leu2 met15 trp1 ura3 HHT1(K56A) HHT2(K56A) pob3(Q308K):KanMX*
Bottom panel	
DY150	*MAT**a** ade2 can1 his3 leu2 trp1 ura3*
DY16281	*MAT**a** ade2 can1 his3 leu2 trp1 ura3 HHT1(K56Q) HHT2(K56Q)*
DY16302	*MAT**a** ade2 can1 his3 leu2 trp1 ura3 HHT1(K56R) HHT2(K56R)*
DY7815	*MAT**a** ade2 can1 his3 leu2 lys2 trp1 ura3 spt16-11*
DY17550	*MAT**a** ade2 can1 his3 leu2 lys2 trp1 ura3 HHT1(K56Q) HHT2(K56Q) spt16-11*
DY17552	*MAT**a** ade2 can1 his3 leu2 met15 ura3 HHT1(K56R) HHT2(K56R) spt16-11*

Table S1; Strains used in Figure S2A; FACT mutations with *hst3*Δ *hst4*Δ

Strain	Genotype
DY150	*MAT**a** ade2 can1 his3 leu2 trp1 ura3*
DY16264	*MAT**a** ade2 can1 his3 leu2 trp1 ura3 hst3Δ:HIS3 hst4Δ:KANMX*
DY19125	*MAT**a** ade2 can1 his3 leu2 lys2 met15 trp1 ura3 pob3(Q308K):LEU2*
DY18250	*MAT**a** ade2 can1 his3 leu2 trp1 ura3 pob3(Q308K):LEU2 hst3Δ:HIS3 hst4Δ:KanMX*
DY18243	*MAT**a** ade2 can1 his3 leu2 trp1 ura3 lys2-128∂*
DY18246	*MAT**a** ade2 can1 his3 leu2 trp1 ura3 lys2-128∂ hst3Δ:HIS3 hst4Δ:KanMX*
10034-6-2	*MAT**a** ade2 can1 his3 leu2 trp1 ura3 lys2-128∂ spt16-11*
10034-10-3	*MAT**a** ade2 can1 his3 leu2 trp1 ura3 lys2-128∂ hst3Δ:HIS3 hst4Δ:KanMX spt16-11*

Table S1; Strains used in Figure S2B; FACT mutations with *rtt109*Δ

Strain	Genotype
DY18243	*MAT**a** ade2 can1 his3 leu2 trp1 ura3 lys2-128∂*
10035-3-3	*MAT**a** ade2 can1 his3 leu2 trp1 ura3 lys2-128∂ rtt109Δ(::KanMX)*
DY18247	*MAT**a** ade2 can1 his3 leu2 trp1 ura3 lys2-128∂ pob3(Q308K):LEU2*
DY19131	*MAT**a** ade2 can1 his3 leu2 trp1 ura3 lys2-128∂ pob3(Q308K):LEU2 rtt109:KanMX*
10034-6-2	*MAT**a** ade2 can1 his3 leu2 trp1 ura3 lys2-128∂ spt16-11*
10035-6-4	*MATα ade2 can1 his3 leu2 trp1 ura3 lys2-128∂ rtt109-Δ(::KanMX) spt16-11*

Table S1; Strains used in Supplemental Figure S1, H3 western blot

Strain	Genotype
DY5699	*MAT**a** ade2 can1 his3 leu2 lys2 met15 trp1 ura3*
DY12949	*MAT**a** ade2 can1 his3 leu2 lys2 met15 trp1 ura3 asf1::KanMX*
DY13030	*MAT**a** ade2 can1 his3 leu2 lys2 trp1 ura3 rtt109::KanMX*
DY16281	*MAT**a** ade2 can1 his3 leu2 trp1 ura3 HHT1(K56Q) HHT2(K56Q)*
DY16302	*MAT**a** ade2 can1 his3 leu2 trp1 ura3 HHT1(K56R) HHT2(K56R)*
DY16313	*MAT**a** ade2 can1 his3 leu2 lys2 trp1 ura3 HHT1(K56A) HHT2(K56A)*

Table S2; primers used for detecting *HHT1* or *HHT2* mutations.

Name	Target	Sequence
F2899	HHT1	5'-GGTACTGTTGCTTTGAGAGAAATC
F3093	HHT1	5'-CTTGCAAGGCACCGATG
F2901	HHT2	5'-GTACTGTTGCCTTGAGAGAAATT
F2902	HHT2	5'-GATTCTTGCAAAGCACCGATA

Supplementary Figures

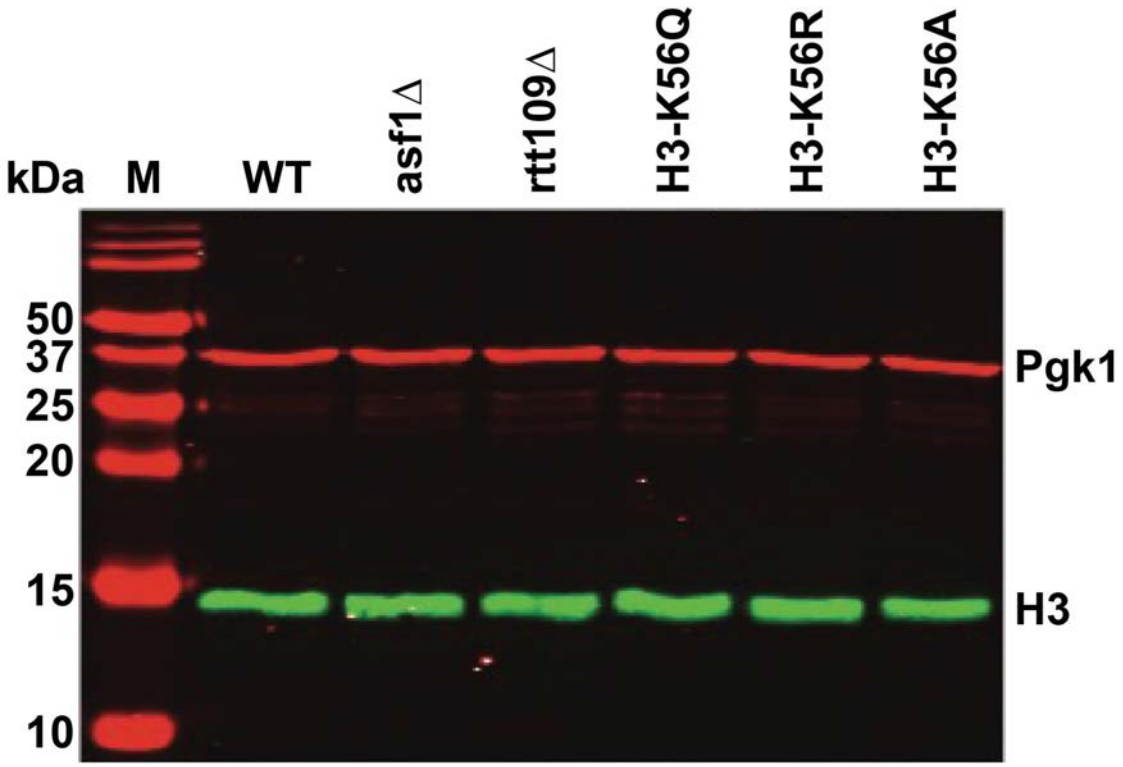

Figure S1 Mutations of H3 did not significantly affect H3 levels

Strains (see Table S1 for full genotypes) were grown to log phase and proteins were extracted by the TCA method (1). A western blot was prepared using 5 µg of lysate from each strain, then the blot was probed with antibodies against histone H3 or Pgk1 as a loading control. Molecular weight standards with approximate sizes in kDa are shown (M, Li-Cor Odyssey One-Color).

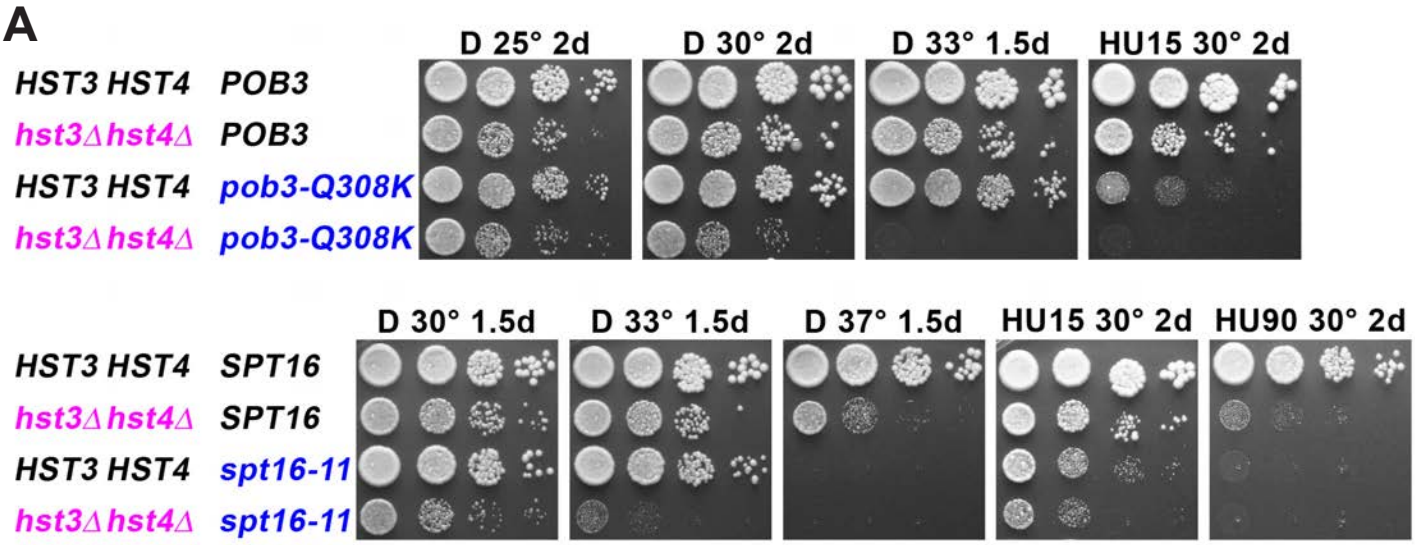

Figure S2 Manipulating H3-K56ac by deleting the HAT and HDACs that regulate this modification reveals genetic interactions with FACT mutants and H3-K56Q.

10-fold serial dilutions of strains (see Table S1) were tested as described in Fig 2. A) FACT mutations tested with deletion of the H3-K56ac deacetylases *HST3* and *HST4*. B) FACT mutations tested with deletion of the H3-H56 acetyltransferase *RTT109*. Growth on –lys (synthetic medium lacking lysine) indicates the Spt⁻ phenotype resulting from incomplete repression of the cryptic promoter associated with insertion of a Ty1 transposon ∂ element in *LYS2* (2). Loss of *RTT109* itself causes HU sensitivity (refs 3-5 and Fig S2B); the dependence of the interaction between Rtt106 and FACT on H3-K56ac (6) makes it difficult to interpret the enhanced HUs.

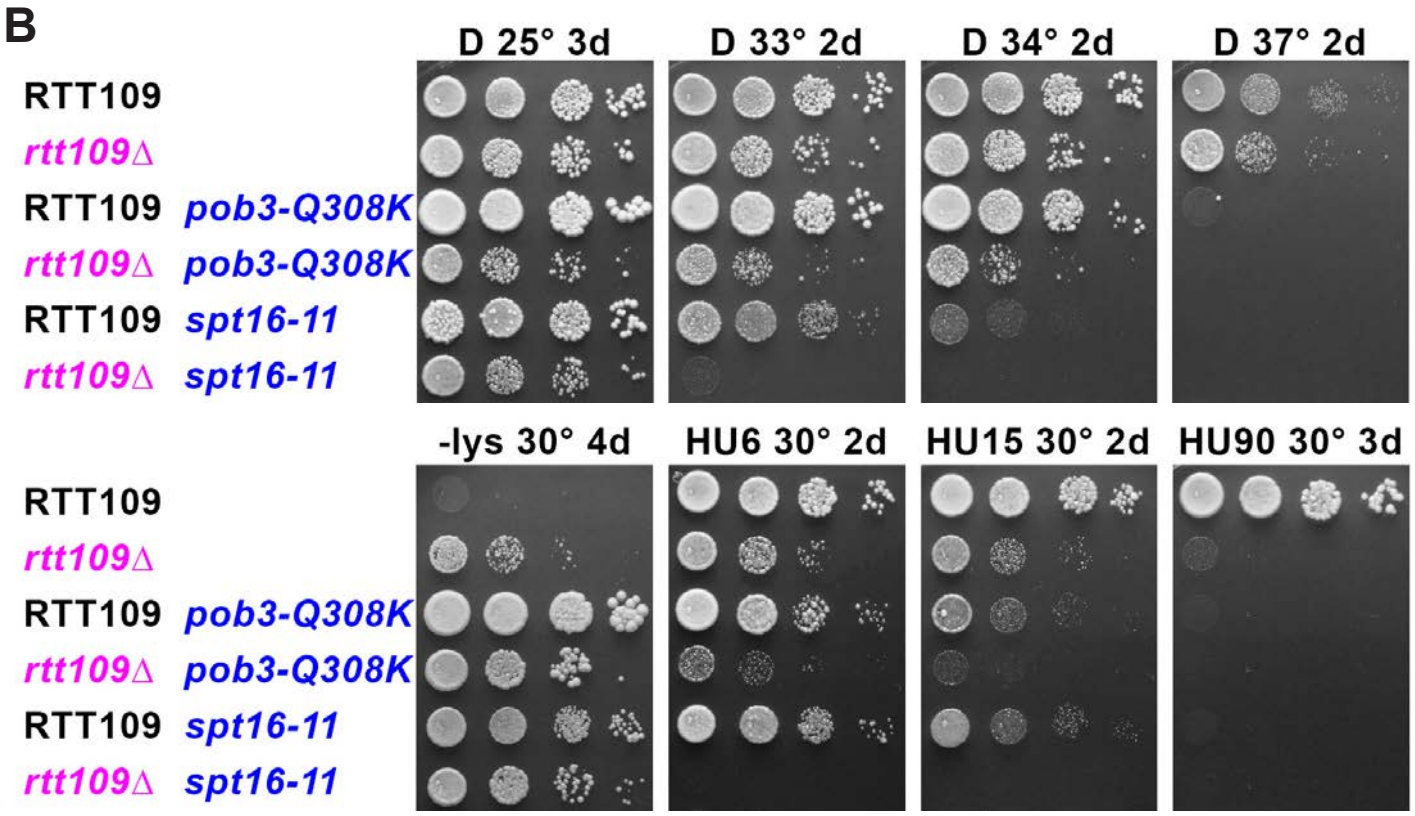

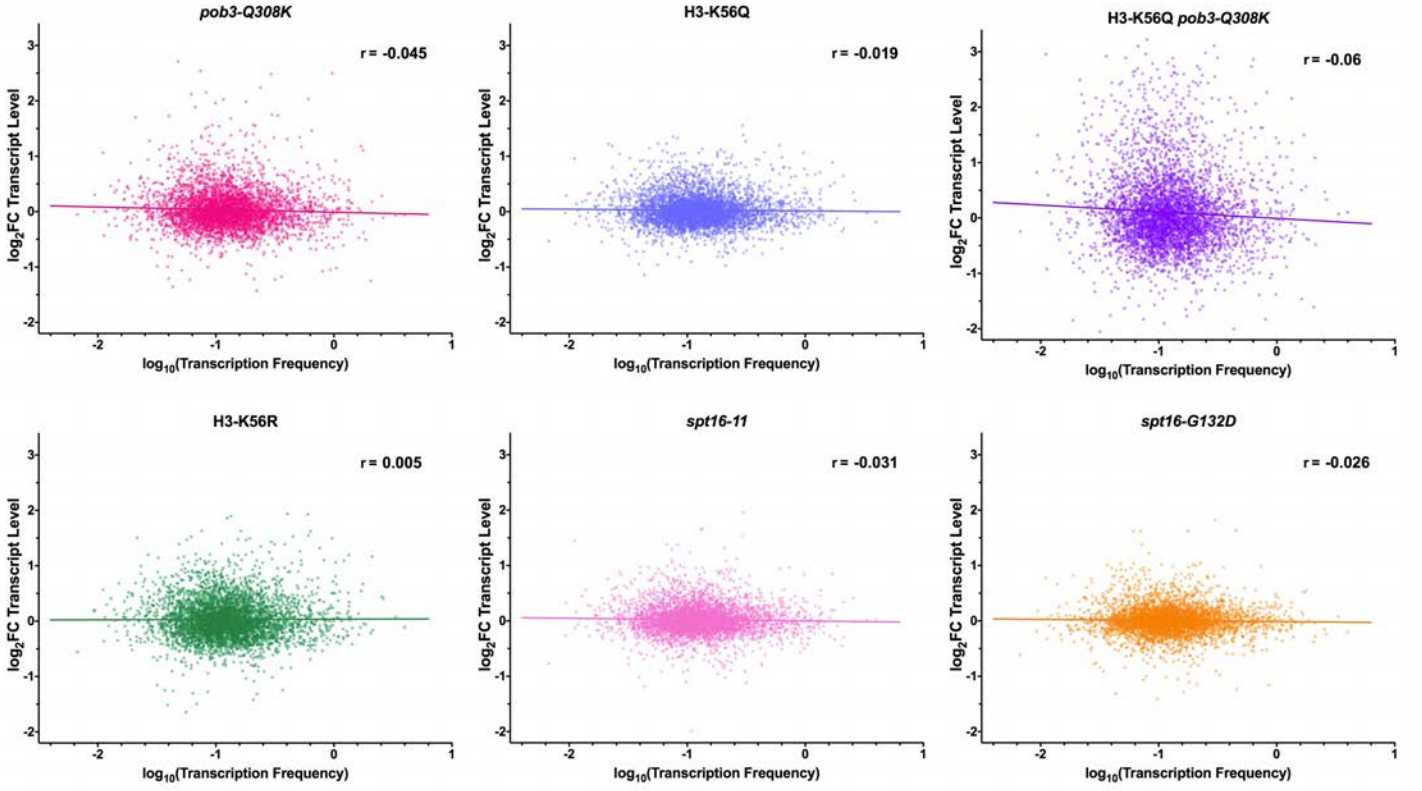

Figure S3A

Transcript level change vs Transcription frequency with all mutations tested. Same as Fig 3B but showing all 6 strains tested; the *pob3-Q308K* panel here is the same as Fig 3B. Results for 4323 genes are shown.

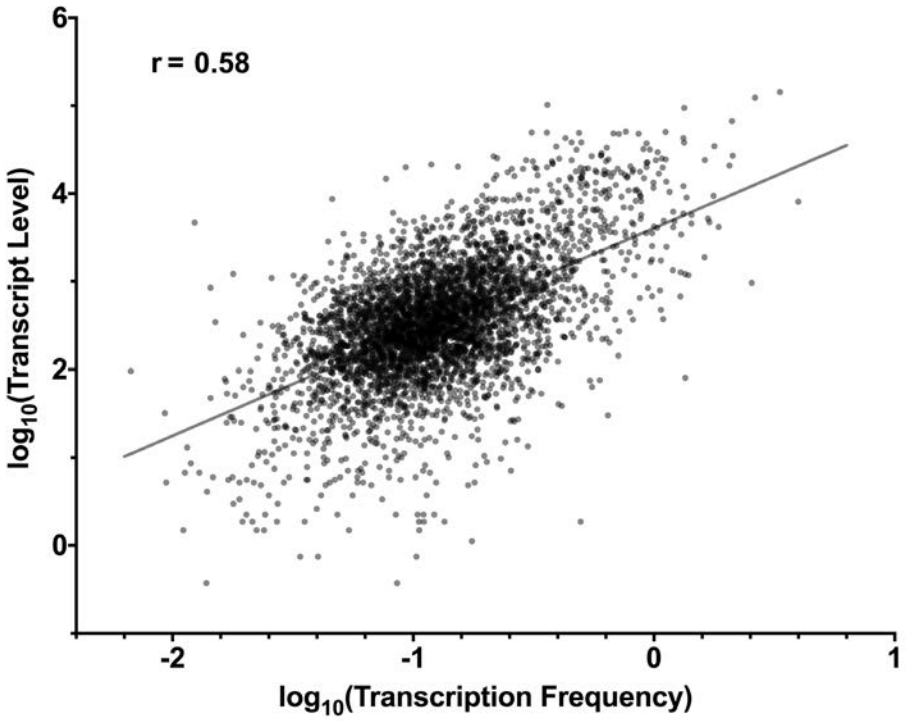

Figure S3B

The correlation between published transcription frequencies and transcript levels in the WT strain in this study. The transcription rates calculated in reference 7 are called “frequencies” here to avoid potential confusion with the rate of progression of RNA Pol II, which was not measured. In this case “rate” refers to the number of transcripts produced per unit of time (reported as mol/min). The calculation takes into account several factors such as transcript stability and RNA Pol II density over genes to provide a more accurate description of the probability of ongoing transcription in each gene. This has advantages over simple counting of transcript levels at steady state, but changes in transcription based on RNA-seq measurements are based on the steady state level of transcripts. As each method of determining the level of transcription has advantages and disadvantages, we report comparisons with each dataset here. Transcription frequency data were available for 4323 genes for which our RNA-seq measurements also produced information (5712 genes). The datasets correlate with one another with a moderately strong Pearson correlation coefficient of 0.58, and yield the regression line shown, indicating that they measure similar but not identical parameters.

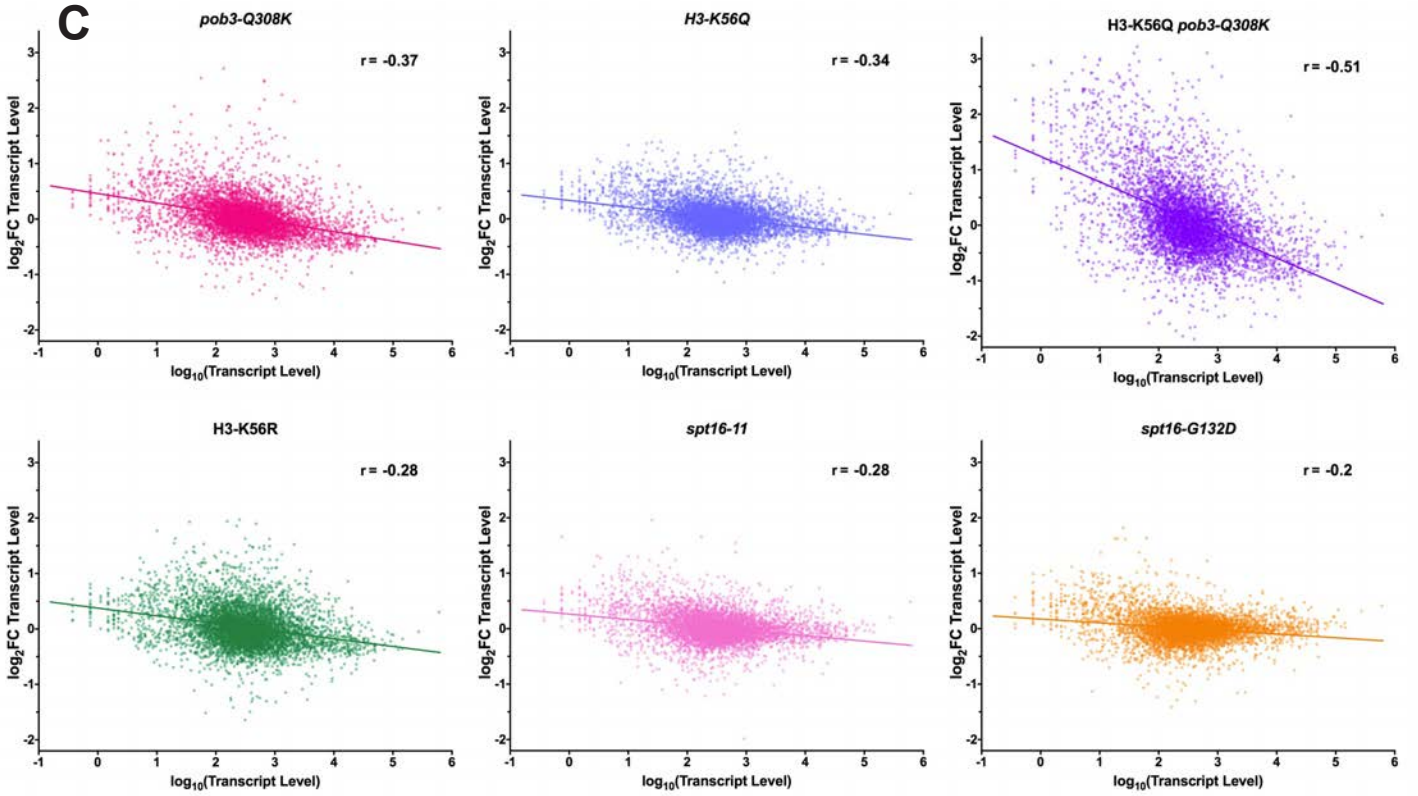

Figure S3C, D Transcript level change vs Transcript level or Gene size in the WT strain with all mutations tested.

Same as Figs 3C, 3D, except showing all 6 strains tested; the *pob3-Q308K* panel is the same as Fig 3C or Fig 3D. Results for 5712 genes are shown.

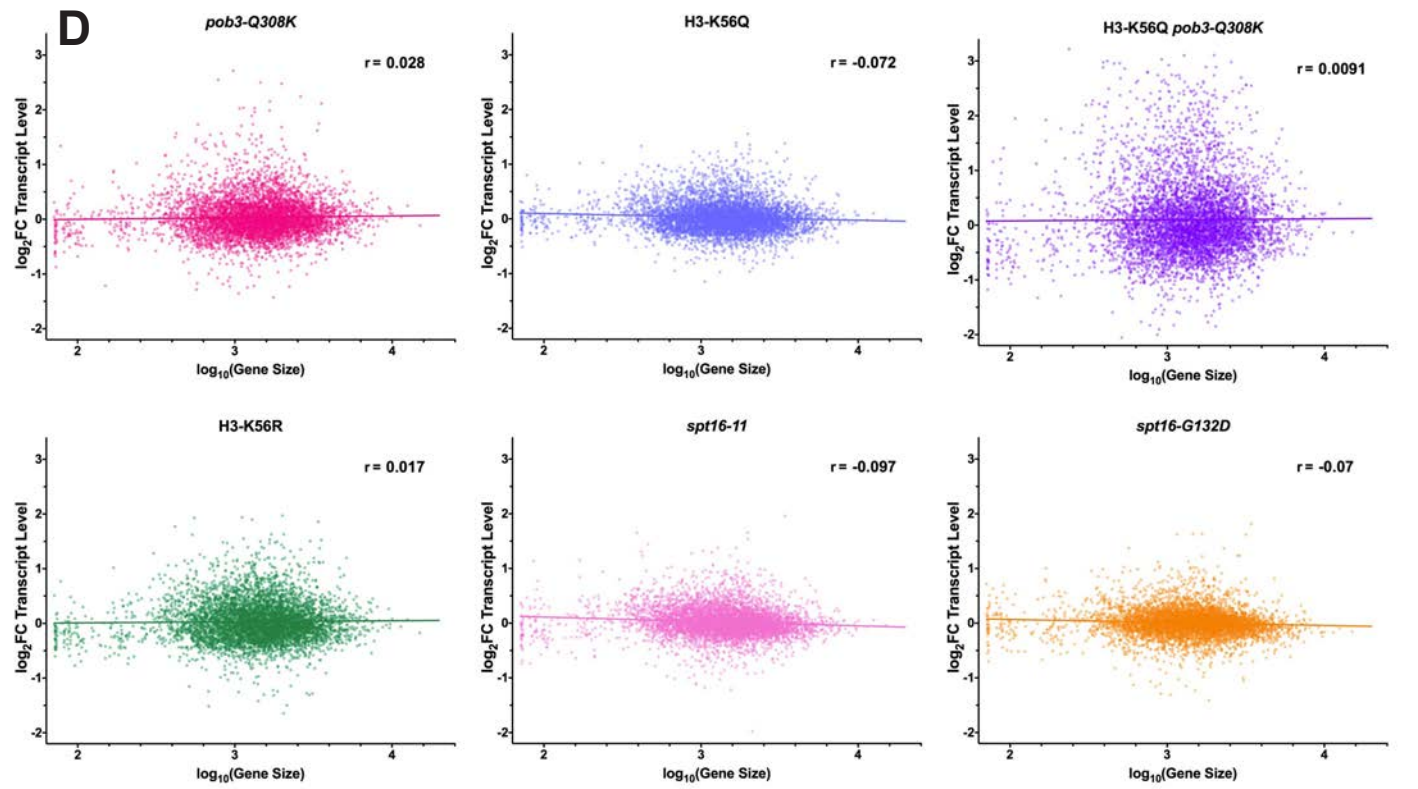

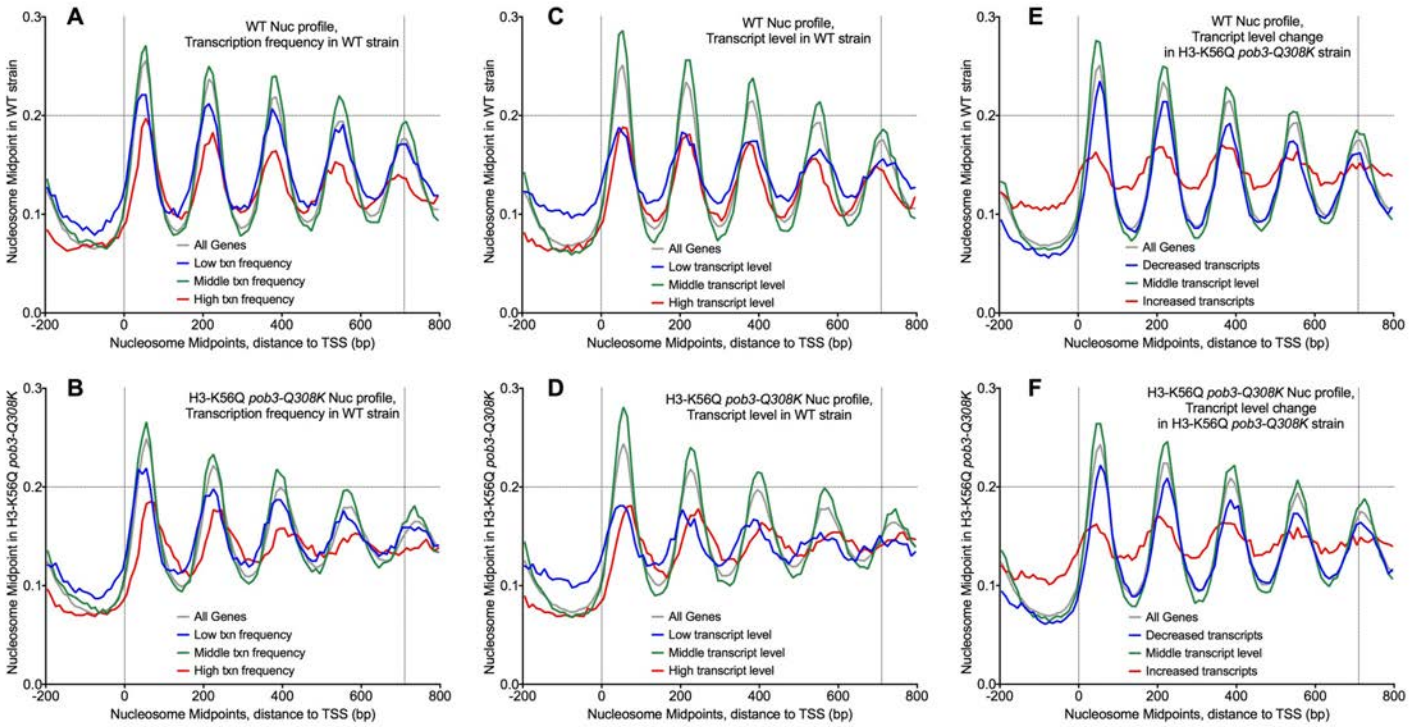

Fig S5A Effects of Transcription and Mutations on Nucleosome positioning

Nucleosome midpoints were called and aligned as in Fig 5A. Three deciles of genes were defined, 0-10th percentile (low or decreased), 45th-55th percentile (middle), and 90th-100th percentile (high or increased; see further analysis of the latter in Fig S6B). Inputs were (A, B) the transcription frequency (7), (C,D) the transcript level from the WT strain used here, or (E,F) the change in transcript level for the H3-K56Q *pob3-Q308K* strain relative to the WT. Nucleosome positioning data for the WT strain are shown in the top panels and for the mutant strain in the bottom panels. Positioning patterns were distinct for highly and lowly transcribed deciles, but similar for WT and mutant strains, aside from the lower coherence and downstream shift noted in Fig 5. Genes with the largest increase in transcription in the mutant had low coherence of positioning, but this was true for both the WT and the mutant.

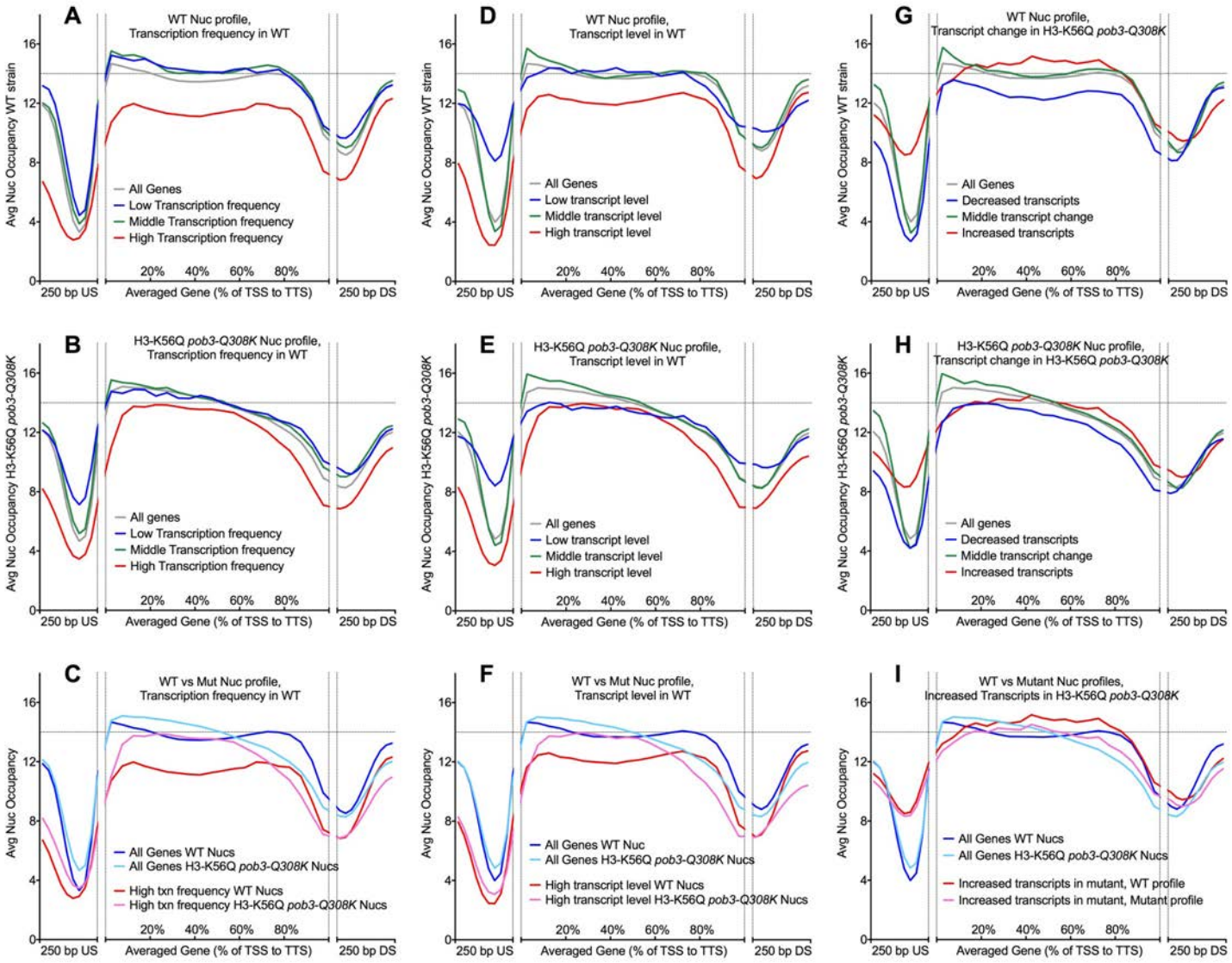

Fig S5B Changes in nucleosome occupancy over the averaged gene do not track with changes in transcription

Deciles of genes were defined as in Fig S5A, then the nucleosome occupancy profiles for normalized gene lengths were plotted as in Fig 5B. Nucleosome profiles are shown for the deciles reflecting high, medium, and low transcription frequencies (A-C), transcript levels (D-F), or increased, unaffected, or decreased transcription in the H3-K56Q *pob3-Q308K* strain (G-I). The nucleosome occupancy in the WT strain is shown in the top row, the mutant in the second row, and the top decile and average for both strains in the bottom row. Panel C shows most clearly the low nucleosome occupancy in highly transcribed genes in the WT and the loss of this feature in the mutant. Panel I shows most clearly that no similar effect is observed when parsing the genes by their change in transcription in the mutant instead of their absolute transcription level.

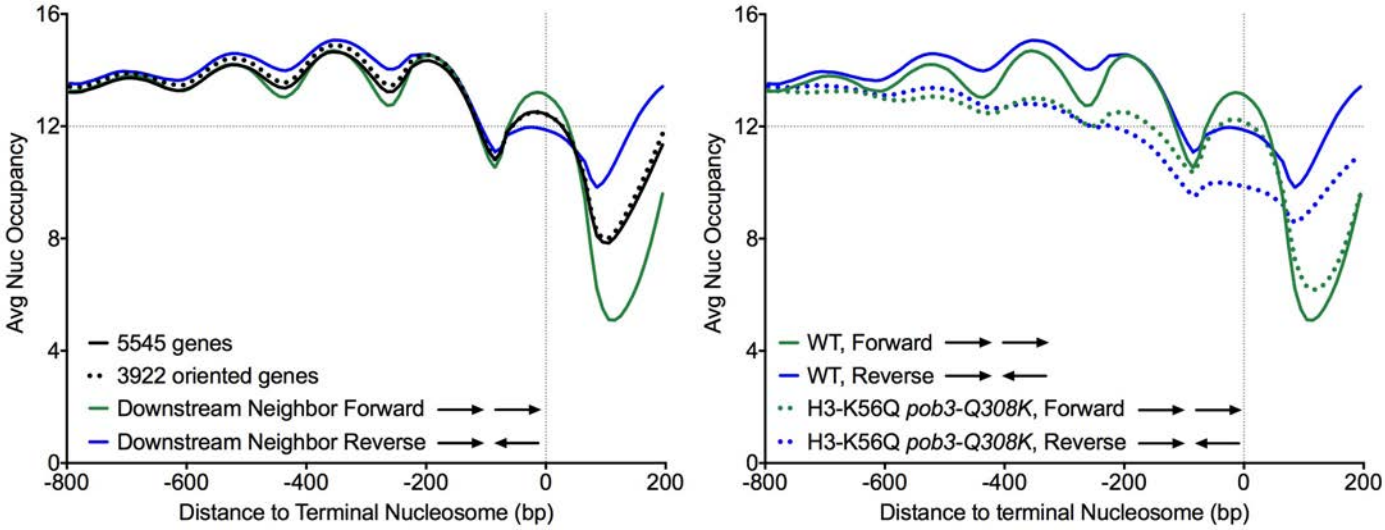

Fig S5C Effects of the orientation of the downstream neighbor on 3' end nucleosome occupancy

Nucleosome occupancy profiles were aligned by the terminal nucleosome for 5545 genes (black line). 3922 of these were readily oriented relative to the neighboring gene downstream, with the dotted line showing that this subset did not have a different nucleosome occupancy profile than the larger group. When separated into genes with downstream neighbors transcribed in the same direction as the target gene (the downstream region is the promoter for the neighbor) and those with converging transcription (the downstream region is the termination site for both genes), distinctive patterns were observed consistent with parallel genes having their promoter in the region downstream of the target gene. This class had higher terminal nucleosome occupancy and lower downstream occupancy, with the opposite being observed with convergent gene orientation. The NDR observed downstream of averaged genes is therefore primarily due to promoters of adjacent genes. These patterns were also observed in the mutant strain, albeit with lower overall occupancy as noted in Fig 5C (right panel), and comparing deciles ordered as in Figs S5A, B did not reveal any distinction (not shown).

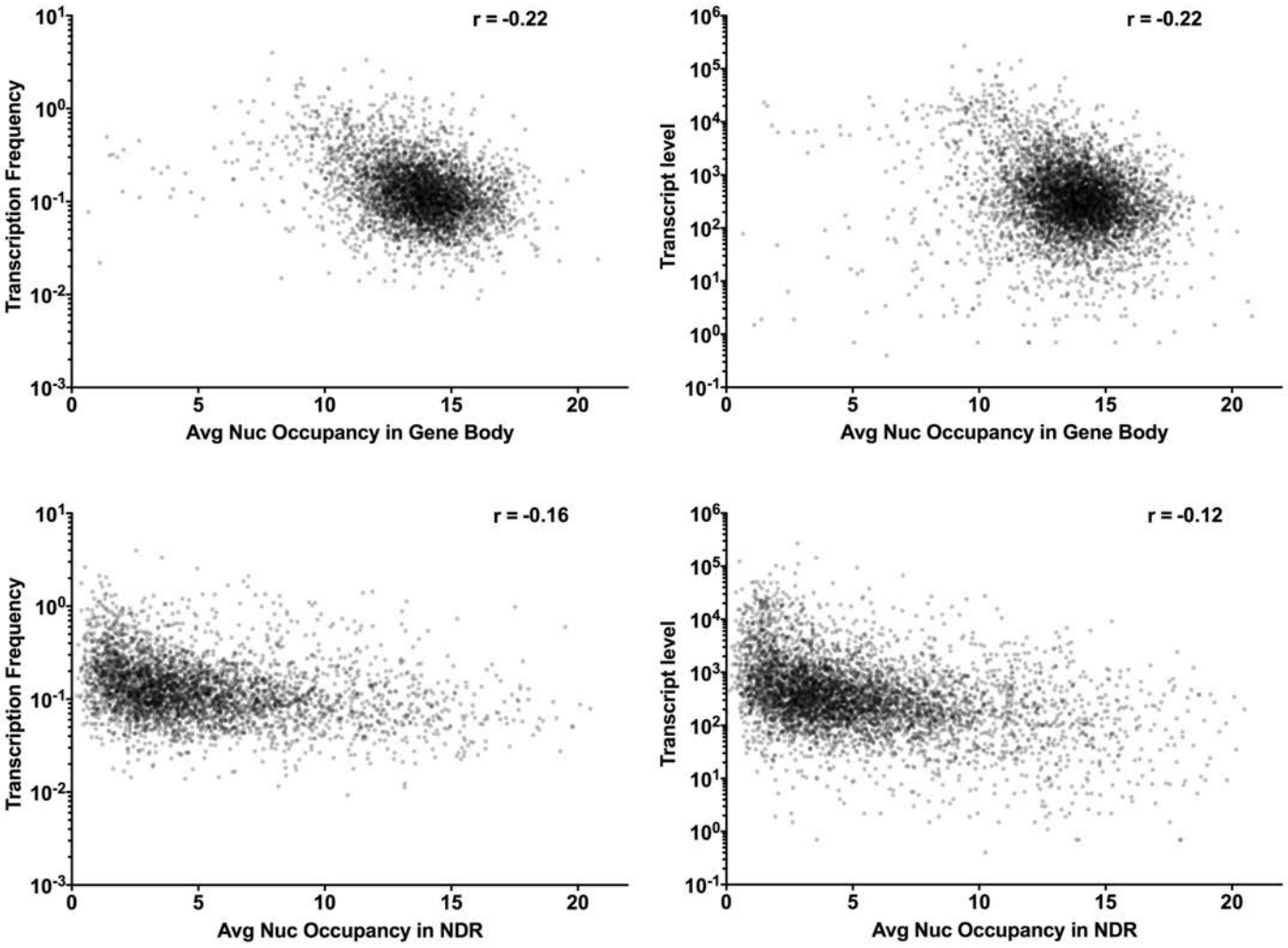

Fig S6A Changes in transcription compared with nucleosome occupancy in a WT

The average nucleosome occupancy was determined for gene bodies (top panels) or NDRs (bottom panels) as in Fig 6, then plotted against the WT transcription frequency or the transcript level in the WT strain from this dataset. Pearson correlation coefficients are shown for each plot, revealing low-moderately low correlations between nucleosome occupancy and transcription frequency in either the NDR or gene body.

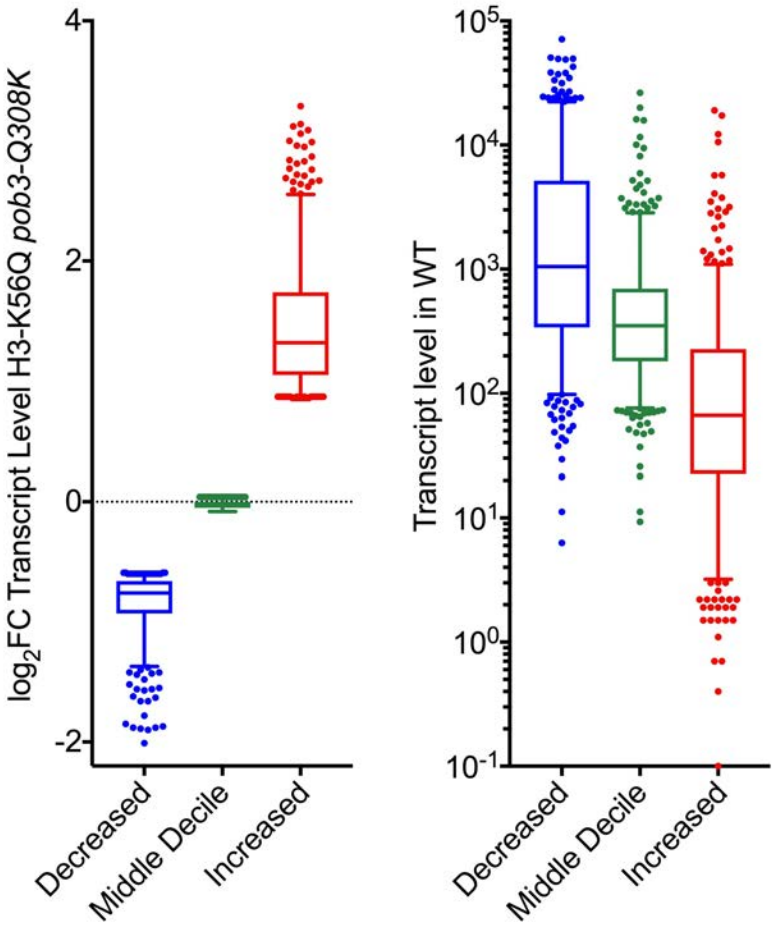

Fig S6B Characterization of deciles used for analysis of changes in transcription

The log_2FC distributions for the deciles based on transcription changes in the H3-K56Q *pob3-Q308K* strain described in Figs S5A and S5B are shown (left panel), along with the absolute transcript levels for these classes in the WT strain (right panel). The variation in transcript levels is high for each class, but overall the decile with the greatest decrease in transcription in the mutant had the highest average transcript level, and the decile with the greatest increase had the lowest average transcript level. While the correlation is weak, this suggests that the mutant lost the ability to maintain each extreme of transcriptional control, causing genes to trend toward more moderate levels of transcription.

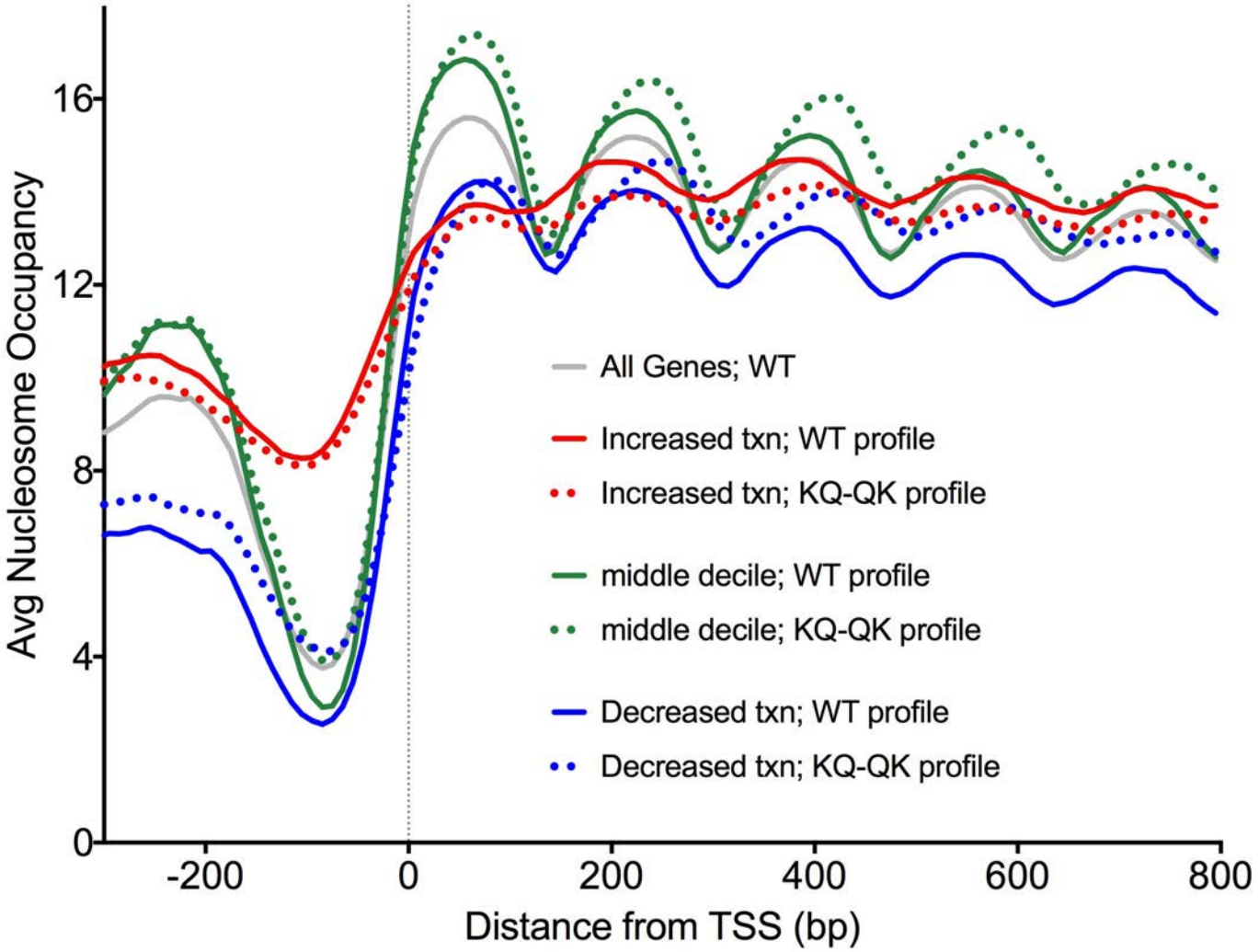

Fig S6C

Nucleosome occupancy results were aligned by the TSS as in Fig 5C, and parsed into three deciles as for Fig S6B according to the change in transcription in the H3-K56Q *pob3-Q308K* mutant. The average for all genes in the WT is shown in grey for reference. This shows that genes whose transcription increased the most in the mutant strain had higher than normal occupancy upstream of the TSS and lower than normal +1 nucleosome occupancy. Genes whose transcription decreased the most also lacked prominent +1 nucleosomes, but had strong NDRs. These patterns were not strongly affected in the mutant, suggesting that these average architectural features defined the classes of genes but did not reveal the drivers of changes in transcription.

Supplementary References

1. McCullough, L., Z. Connell, C. Petersen, and T. Formosa, *The Abundant Histone Chaperones Spt6 and FACT Collaborate to Assemble, Inspect, and Maintain Chromatin Structure in Saccharomyces cerevisiae.* Genetics, 2015. **201**(3): p. 1031-45. PMID: 26416482; PMC4649633.
2. Simchen, G., F. Winston, C.A. Styles, and G.R. Fink, *Ty-mediated gene expression of the LYS2 and HIS4 genes of Saccharomyces cerevisiae is controlled by the same SPT genes.* Proc Natl Acad Sci USA, 1984. **81**: p. 2431-2434.
3. Schneider, J., P. Bajwa, F.C. Johnson, S.R. Bhaumik, and A. Shilatifard, *Rtt109 is required for proper H3K56 acetylation: a chromatin mark associated with the elongating RNA polymerase II.* J Biol Chem, 2006. **281**(49): p. 37270-4. PMID: 17046836.
4. Driscoll, R., A. Hudson, and S.P. Jackson, *Yeast Rtt109 promotes genome stability by acetylating histone H3 on lysine 56.* Science, 2007. **315**(5812): p. 649-52. PMID: 17272722; 3334813.
5. Han, J., H. Zhou, B. Horazdovsky, K. Zhang, R.M. Xu, and Z. Zhang, *Rtt109 acetylates histone H3 lysine 56 and functions in DNA replication.* Science, 2007. **315**(5812): p. 653-5. PMID: 17272723.
6. Li, Q., H. Zhou, H. Wurtele, B. Davies, B. Horazdovsky, A. Verreault, and Z. Zhang, *Acetylation of histone H3 lysine 56 regulates replication-coupled nucleosome assembly.* Cell, 2008. **134**(2): p. 244-55. PMID: 18662540; PMC2597342.
7. Pelechano, V., S. Chavez, and J.E. Perez-Ortin, *A complete set of nascent transcription rates for yeast genes.* PLoS One, 2010. **5**(11): p. e15442. PMID: 21103382; PMC2982843.